PACS numbers: 42.55.Rz; 42.55.Xi; 42.60.Lh; 42.70.Hj
DOI: 10.1070/QE2005v035n12ABEH004094

Longitudinally diode-pumped quasi-continuous Yb^{3+}, Er^{3+} : LSB laser

Yu.P. Rudnitskii, L.V. Shachkin, S.T. Durmanov, G.V. Smirnov

***Abstract*. A quasi-continuous output power of 1.1 W is generated at 1.56 μm in a longitudinally pumped Yb^{3+}, Er^{3+} : $LaSc_3(BO_3)_4$ (Yb, Er : LSB) crystal. The lasing efficiencies of the Yb, Er : LSB laser and Er : phosphate glass laser are compared under the same pump conditions.**

Keywords: *LSB crystal, longitudinal pumping, thermal deformations, quasi-continuous lasing.*

1. Introduction

Phosphate glasses doped with Er^{3+} and Yb^{3+} ions are at present the best material for erbium lasers emitting at $\sim$ 1.5 μm. The main substantial disadvantages of this glass are its low heat conduction and low thermomechanical damage threshold. For this reason, various thermal effects restrict the average output power of erbium lasers [1, 2]. Crystals doped with Er^{3+} and Yb^{3+} ions have a higher heat conduction compared to that of a phosphate glass, however, the lasing efficiency of most of them is considerably lower than in a phosphate glass due to a longer lifetime of the $^4I_{11/2}$ level of the Er^{3+} ion and, as a rule, a lower stimulated emission cross section. Because lasers emitting at 1.5 μm can be used for a number of practical applications, active work is permanently underway on the improvement of optical and thermomechanical properties of glasses [3 – 6] and the search for new crystals [7 – 15].

A crystal pretending to the role of the main material for the active element of a diode-pumped erbium laser is lanthanum-scandium borate $LaSc_3(BO_3)_4$ (LSB) [8], in which the lifetime of the $^4I_{11/2}$ level of the Er^{3+} ion is shorter than that in phosphate glasses. One of the most important disadvantages of an LSB crystal is the much shorter lifetime of the $^4I_{13/2}$ upper laser level of the Er^{3+} ion ($\sim$ 700 μs) compared to that in the glass, which requires high pump rates. Despite a comparatively low heat conduction ($\sim$ 2.8 W m^{-1} K^{-1}) and an order of magnitude shorter lifetime of the $^4I_{13/2}$ level of the Er^{3+} ion compared to that in phosphate glasses [13], the $\sim$ 150-mW cw output power was obtained in this crystal [12], which today, to our knowledge, is second only to the result obtained in paper [15] where 250 mW of cw lasing at 1.55 μm was achieved in the fundamental TEM_{00} mode in the Er^{3+}, Yb^{3+} : $YCa_4O(BO_3)_3$ crystal. In [12, 15], pumping was performed by $\sim$ 1.5-W diode lasers with fibre pigtails.

In this paper, we compared the efficiencies of the Yb^{3+}, Er^{3+}: LSB laser and erbium phosphate glass laser in a quasi-continuous regime longitudinally pumped by a 30-W diode bar.

2. Experimental

Figure 1 shows the optical scheme of the experimental setup. Pumping was performed by a 25-W, 976-nm cw LIMO diode bar (Dortmund, Germany). The diode bar was used in experiments as a quasi-continuous radiation source emitting pulses of duration up to 5 ms and power up to 30 W. The diode bar was mounted on a Peltier thermoelectric element, which was used for temperature tuning of the diode bar radiation wavelength. The collimated radiation of the bar was focused with a spherical lens on the input face of an active element.

We studied the active element made of an LSB crystal with concentrations $[Yb] = 1.35 \times 10^{21}$ cm^{-3} and $[Er] = 6.7 \times 10^{19}$ cm^{-3}, which was grown by S.A. Kutovoi. The

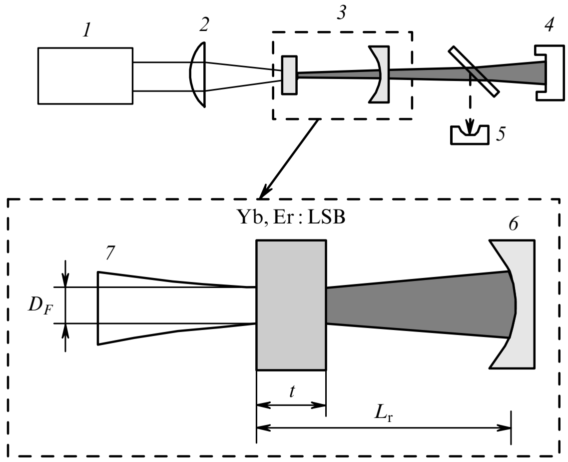

Figure 1. Scheme of the experimental setup: (*1*) diode bar; (*2*) lens; (*3*) resonator with an active element; (*4*) power meter; (*5*) germanium photodiode; (*6*) resonator mirror; (*7*) pump radiation; (*t*) crystal thickness.

Yu.P. Rudnitskii, L.V. Shachkin, S.T. Durmanov, G.V. Smirnov State Scientific Center of the Russian Federation, Troitsk Institute for Innovation and Fusion Research, 142190 Troitsk, Moscow region, Russia; e-mail: smirgen@triniti.ru

Received 11 March 2005; revision received 13 October 2005
Kvantovaya Elektronika **35** (12) 1113 – 1116 (2005)
Translated by M.N. Sapozhnikov

active element was a 2-mm thick plane–parallel plate cut from the crystal perpendicular to its z axis. One of the crystal faces was covered with a multilayer dielectric coating with the reflectance $R = 99.8\,\%$ at 1.5 μm and the transmission coefficient $T > 96\,\%$ at 975 nm. This face was used as the resonator mirror through which the active element was pumped. To reduce resonator losses at 1.5 μm, an AR coating was deposited on another face of the active element. The spectral region with the absorption coefficient admissible for longitudinal pumping ($k \approx 8.5$ cm^{-1} for the $\boldsymbol{E} \perp z$ polarisation [13]) lies between 970 and 982 nm. The active element was pumped by the diode bar at 973 nm. The fraction α of the pump radiation absorbed in the active element was measured to be ~ 0.8.

The active element made of a phosphate glass (fabricated at the Institute of Radio Engineering and Electronics, RAS and donated by A.A. Izyneev) with concentrations $[\mathrm{Yb}] = 2.2 \times 10^{21}$ cm^{-3} and $[\mathrm{Er}] = 8 \times 10^{19}$ cm^{-3} was a 3-mm thick 6×6 mm plane–parallel plate. Both faces of the plate were covered with multilayer dielectric coatings. One face (6×6 mm) with the reflectance $R = 99.8\,\%$ at 1.5 μm and the transmission coefficient $T > 97\,\%$ at 970 nm served as the resonator mirror through which the active element was pumped. To use the pump radiation more efficiently, a coating with the reflectance 99 % at 970 nm was deposited on another face; in this case, transmission at the lasing wavelength exceeded 97 %. The active element was pumped at 969 nm by the diode bar cooled down to 6 °C.

Because the radiation divergences along the fast and slow axes of the diode bar were somewhat different, the pump radiation spot on the input face had the shape of an ellipse with the axial ratio $\sim 1:1.4$. The focal spot diameter D_F of pump radiation presented below corresponds to the minor axis of the ellipse. The values of D_F were determined for the half-maximum intensity. The cross section of the waist of the focused pump radiation was virtually constant over the entire length of the active element for all lenses used in experiments.

The optimal lasing regimes were found for both lasers by varying the pump intensity I_{p}, the resonator length L_{r}, the radius of curvature r, and the reflectance R_{out} of the output mirror in a broad range. All the results were obtained at a pulse repetition rate of ~ 1 Hz. The active elements were not cooled.

3. Results

The LSB active element was pumped by pulses of duration considerably exceeding the lifetime $\tau_{\mathrm{up}} \approx 700$ μs of the upper laser level of the Er^{3+} ion [13]. Because of a relatively short lifetime τ_{up} and the low cross section for stimulated emission, the threshold pump intensity I_{th} was higher than 10 kW cm^{-2}. The maximum lasing efficiency was observed in the resonator with a plane mirror with the reflectance $R_{\mathrm{out}} = 97.2\,\%$ (the highest reflectance for the mirrors available). As the transmission of the output mirror was increased from 2.8 % to 5 %, not only the value of I_{th} almost doubled but also the output laser power drastically decreased (approximately by an order of magnitude). The optimal pump intensity I_{p} corresponding to the maximum output power proved to be so high ($I_{\mathrm{p}} \approx 25$ kW cm^{-2} for $D_F \approx 300$ μm) that thermal deformations of the active element during the action of the pump pulse τ_{p} considerably affected the lasing process. Figure 2 shows the oscillograms of output pulses for resonators of different lengths. One can see that a relatively stable quasi-continuous lasing during the entire 4-ms pulse was obtained only in the resonator with the shortest length. Figure 3 shows the dependence of E_{out} on τ_{p} for the maximum power $P_{\mathrm{p}} = 30.7$ W. It follows from Fig. 3 that the output power in the quasi-continuous regime is $P_{\mathrm{out}} = 1.1$ W. The maximum optical efficiency $\eta_{\mathrm{op}} = E_{\mathrm{out}}/(P_{\mathrm{p}} \alpha \tau_{\mathrm{p}})$ obtained in this case is $\sim 4.0\,\%$ and the maximum slope efficiency is $\eta \approx 4.6\,\%$.

The best results for the phosphate glass active element were obtained for $D_F \approx 500$ μm. Figure 4 shows the shapes of the output pulse and current pulse of the diode bar power supply in this case. The dependence of the output energy E_{out} on the energy E_{abs} absorbed in the active element for

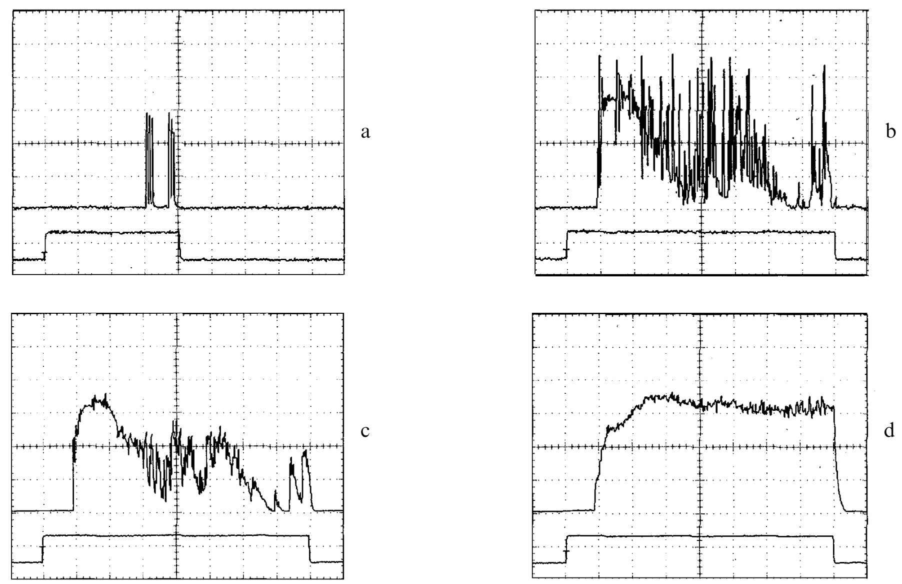

Figure 2. Oscillograms of the output pulses of the Yb, Er : LSB laser (upper traces) and of pump pulses (lower traces) for $L_{\mathrm{r}} = 30$ mm (one pulse) (a), 13 mm (one pulse) (b), 13 mm (averaged over 16 pulses) (c), and 4 mm (averaged over 16 pulses) (d), $P_{\mathrm{p}} = 30.7$ W, $r = \infty$, $R_{\mathrm{out}} = 97.2\,\%$.

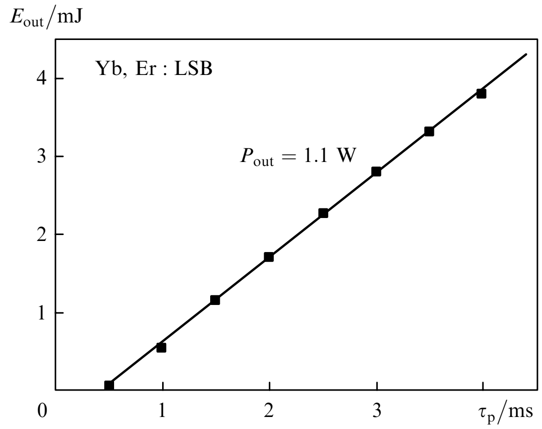

Figure 3. Dependence of the output laser energy E_{out} on the pump pulse duration τ_p for the maximum power $P_p = 30.7$ W, $r = \infty$, $R_{out} = 97.2$ % and $L_r = 4$ mm.

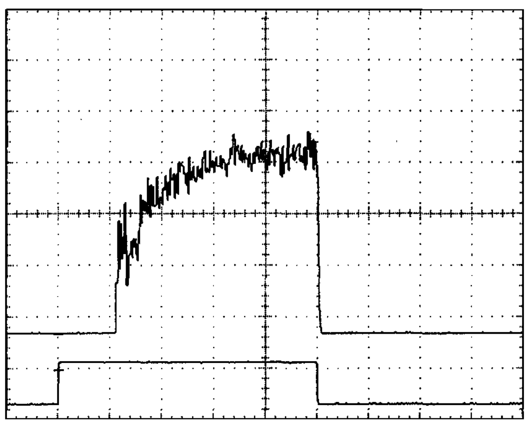

Figure 4. Oscillograms of the output pulse of the Yb, Er phosphate glass laser (upper trace) and of the pump pulse (lower trace) for $P_p = 30.7$ W, $r = \infty$, $R_{out} = 95$ % and $L_r = 30$ mm (averaged over 16 pulses).

the pump power $P_p = 30.7$ W is shown in Fig. 5. In this case, the maximum optical efficiency is $\eta_{op} \approx 13.3$ %, the maximum slope efficiency is $\eta \approx 20$ %, and the quasi-cw output power is ~ 6 W. For comparison, the dependence of E_{out} on E_{abs} obtained for the Yb, Er : LSB laser for the same value of P_p is also presented in Fig. 5.

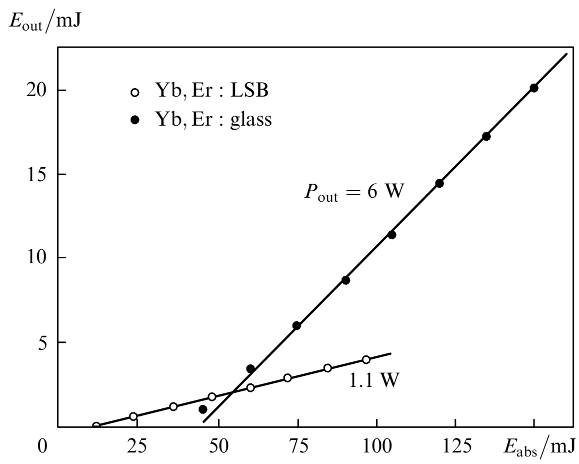

Figure 5. Dependences of the output energy E_{out} on the energy E_{abs} absorbed in the active element for the Yb, Er : LSB laser and the Yb, Er phosphate glass laser for the pump power $P_p = 30.7$ W.

4. Conclusions

We have compared the efficiencies of longitudinally pumped lanthanum-scandium borate crystal and phosphate glass lasers by using pump parameters (pump radiation power $P_p \approx 30$ W and pump pulse duration $\tau_p = 1 - 5$ ms) close to those required for obtaining Q-switching with the output energy $E_{md} \gtrsim 1$ mJ [16]. Although the temperature conductivity of the LSB crystal $\chi \approx 0.013$ cm^2 s^{-1} exceeds that of the phosphate glass almost by a factor of four and the characteristic heat transfer length $L_h \approx 2(\chi\tau_p)^{1/2}$ for the time $\tau_p = 4$ ms is of the order of the pump focal spot radius, the heat release in the LSB active element during the pump pulse causes a stronger deformation of the active element surface. By using the method [17] for measuring the focal distance of a thermal lens in solid-state lasers with a short active medium, which is based on the observation of generation quenching, we estimated the curvature of the active element surface representing the resonator mirror. According to our estimates, the radius of curvature of the LSB active element to the end of the 30-W, 2-ms pump pulse was $r_c \approx 15$ mm, being more than an order of magnitude smaller than r_c for the phosphate glass active element.

As shown above, the quasi-cw lasing efficiency of the LSB laser was several times lower than that of the phosphate glass laser. This circumstance and the fact that a small increase in radiation losses on the output mirror of the resonator of the LSB laser resulted in the decrease in the output power by an order of magnitude suggest that the efficiency of the longitudinally pumped Q-switched Yb, Er : LSB laser will be also very low.

Acknowledgements. The authors thank A.A. Izyneev and P.I. Sadovskii for placing the phosphate glass active element at our disposal.

References

1. Laporta P., Taccheo S., Longhi S., Svelto O., Svelto C. *Opt. Mater.*, 11, 269 (1999).
2. Cai Z.P., Chardon A., Xu H., Feron P., Stephan G.M. *Opt. Commun.*, 203, 301 (2002).
3. Jiang S., Myers J., Wu R., Gregg M., Bishop M., Phonehouse D., Myers M., Hamlin S. *Proc. SPIE Int. Soc. Opt. Eng.*, **2379**, 17 (1995).
4. Denker B.I., Galagan B.I., Osiko V.V., Sverchkov S.E. *Laser Phys.*, **12**, 104 (2002).
5. Alekseev N.E., Byshevskaya-Konopko L.O., Vorob'ev I.L., Izyneev A.A., Sadovskii P.I. *Kvantovaya Elektron.*, **33**, 1062 (2003) [*Quantum Electron.*, **33**, 1062 (2003)].
6. Wu R., Myers J.D., Myers M.J. *Proc. SPIE Int. Soc. Opt. Eng.*, **4968**, 11 (2003).
7. Denisov A.L., Zharikov E.V., Zagumennyi A.I., Kalitin S.P., Smirnov V.A., Talybov A.I., Shcherbakov I.A. *Zh. Prikl. Spektr.*, **49**, 430 (1988).
8. Kutovoi S.A., Laptev V.V., Matsnev S.Yu. *Kvantovaya Elektron.*, **18**, 149 (1991) [*Sov. J. Quantum Electron.*, 21, 131 (1991)].
9. Schweizer T., Jensen T., Heumann F., Huber G. *Opt. Commun.*, **118**, 557 (1995).
10. Simondi-Teisseire D., Viana B., Lejus A., Benitez J., Vivien D., Borel C., Templier R., Wyon C. *IEEE J. Quantum Electron.*, **32**, 2004 (1996).

11. Capobianco J.A., Kabro P., Ermeneux F.S., Moncorge R., Bettinelli M., Cavalli E. *Chem. Phys.*, **214**, 329 (1997).
12. Diening A., Heumann F., Huber G., Kuzmin O. *Techn. Dig. on CLEO'98* (USA, Washington: OSA, 1998) Paper CWM-5, Vol. 7.
13. Lebedev V.A., Pisarenko V.F., Selina N.V., Perfilin A.A., Brik M.G. *Opt. Mater.*, **14**, 121 (2000).
14. Voroshilov I.V., Lebedev V.A., Ignatiev B.V., Gavrilenko A.N., Isaev V.A., Pisarenko V.F. *J. Phys.: Condens. Mater.*, **12**, L287 (2000).
15. Burns P., Dawes J.M., Wang P., Piper J.A., Zhang H., Zhu L., Meng X. *Proc. SPIE Int. Soc. Opt. Eng.,* **4968**, 79 (2003).
16. Boutchenkov V., Kuchma I., Levoshkin A., Mak A., Petrov A., Hollemann G. *Opt. Commun.*, **177**, 383 (2000).
17. Vedyashkin N.V., Derzhavin S.I., Kuz'minov V.V., Mashkovskii D.A. *Kvantovaya Elektron.*, **33**, 367 (2003) [*Quantum Electron.*, **33**, 367 (2003)].